

## Article

# A UAV-Based Forest Fire Patrol Path Planning Strategy

Yiqing Xu <sup>1</sup> , Jiaming Li <sup>2</sup> and Fuquan Zhang <sup>2,\*</sup><sup>1</sup> School of IT and Software, Nanjing Vocational University of Industry Technology, Nanjing 210023, China<sup>2</sup> College of Information Science and Technology, Nanjing Forestry University, Nanjing 210037, China

\* Correspondence: zfq@njfu.edu.cn

**Abstract:** The application of UAVs in forest fire monitoring has attracted increasing attention. When a UAV carries out forest fire monitoring cruises in a large area of the forest, one of the main problems is planning an appropriate cruise path so that the UAV can start from the starting point, cruise the entire area with little detour, and return to the initial position within its maximum cruise distance. In this paper, we propose a flight path planning method for UAV forest fire monitoring based on a forest fire risk map. According to the forest fire risk level, the method uses the ring self-organizing mapping (RSOM) algorithm to plan a corresponding flight path. In addition, since it is difficult for a single UAV to complete a single full-path cruise task in a large area within its maximum cruise time, a multi-UAV cruise scheme is proposed. First, the Gaussian mixture clustering algorithm is used to cluster the study area and divide it into several subareas. In combination with the RSOM algorithm, the corresponding path is planned for each UAV. A simulation with an actual dataset showed that the proposed method solves the problem of UAV patrol path planning for forest fire monitoring and can complete the task within a reasonable time.

**Keywords:** fire risk map; flight path; multi-UAV

**Citation:** Xu, Y.; Li, J.; Zhang, F. A UAV-Based Forest Fire Patrol Path Planning Strategy. *Forests* **2022**, *13*, 1952. <https://doi.org/10.3390/f13111952>

Academic Editor: William W. Hargrove

Received: 31 August 2022

Accepted: 16 November 2022

Published: 18 November 2022

**Publisher's Note:** MDPI stays neutral with regard to jurisdictional claims in published maps and institutional affiliations.



**Copyright:** © 2022 by the authors. Licensee MDPI, Basel, Switzerland. This article is an open access article distributed under the terms and conditions of the Creative Commons Attribution (CC BY) license (<https://creativecommons.org/licenses/by/4.0/>).

## 1. Introduction

Forest fires cause not only great economic losses but also environmental pollution. Effective forest fire prevention methods can reduce the losses caused by fires [1–3]. In recent years, wireless sensor networks have been used for fire monitoring and early warning. In theory, when many nodes are deployed, a fire can be detected in a timely manner [4–6]. However, forest areas are vast, and the number of nodes that can be deployed is limited by financial budgets. Consequently, it is difficult to cover the whole area with a limited number of deployed nodes.

However, widely used fire watchtowers can cover a large area [7–9], although blind areas still exist due to the influence of terrain variation. Therefore, in the case of large forest areas, constructing an effective monitoring system is of great significance to prevent fires.

Currently, the development of UAV technology has attracted extensive attention [10–12], because it has the potential to collect and transfer real-time images of target areas [13–15]. UAVs, which have a simple structure and flexible flight capability and are low cost, are gradually being used in various fields such as forest fire monitoring [16–18].

In a large forest area, one of the problems with using UAVs is planning an appropriate cruise path. Currently, the UAV path planning problem is usually simplified to the traveling salesman problem [19,20]. Methods such as neural network, genetic algorithm, simulated annealing algorithm, and differential evolution ant colony algorithm can be used to get the optimal path [21,22]. When there are a few places that need to be visited for data acquisition, the differential evolution and hybrid ant colony algorithms can find the shortest patrol path for a UAV route [23–25]. However, in a large forest area, it is difficult to derive the situation of the whole area by traversing the locations of only a limited number of sensor nodes.

Compared with a single UAV, collaborative patrolling with multiple UAVs can improve the corresponding monitoring efficiency [26–28]. Multiple UAVs create multiple patrol

paths from source to destination. The main advantage of using multiple patrol paths is that it reduces the area visited by a single UAV. It also helps in reducing the total patrol time during emergency patrolling. Table 1 provides a comparison of path planning methods in the literature.

However, how to divide the whole area into subareas so that a single UAV can finish its patrol task and return to the initial position within its maximum cruise range and how to determine which places should be visited more frequently are still open for research.

The probability of fire events differs in different regions of a forest. Factors such as topography, climate, human activity, and vegetation are recognized as the main causes of regional fires [29–31]. These factors can influence each other directly or indirectly. For example, an area with steep slope and rugged roads may be a place where few people tread; thus, it will have high vegetation coverage and more combustible materials, but fewer careless fires caused by humans [32–34].

By analyzing the relationship between these factors and historical fire locations, a forest fire risk map can be produced. The forest fire risk map is used to predict the probability of fire occurring in a region, which is crucial for management departments to perform patrolling tasks and allocate fire prevention resources effectively [35–37]. Generally, one of the main purposes of UAV path planning is to design a patrol path directed at a specific target with minimal cost. An important feature of forest fire detection tasks is that routes are created with a focus on increasing the probability of fire detection. Thus, when we plan a UAV patrolling path, areas with different levels of fire probability should adopt different strategies. Otherwise, the UAV resource allocation may not be appropriate, which could reduce detection efficiency.

The random search-based (RSB) method can design a UAV patrol path in the simplest way. It randomly selects the points to be visited, considering whether the UAV can finish the patrol task and return to the initial position within the maximum cruise range. The RSB method can be optimized with fire risk information. The local search-based (LSB) method starts with a randomly created path, and then evaluates the fitness of the path by the total average fire probability of all possible paths. This is a kind of heuristic algorithm that obtains near-optimal paths of a local area by sacrificing optimality and accuracy for speed [38].

**Table 1.** Factors considered in path planning methods in the literature.

Reference	Large Area Suitability	UAV Endurance	Cruise Frequency	Optimization Objective		Multiple UAVs
				Distance	Fire risk	
[13]		✓		✓		
[17,27]	✓	✓		✓		✓
[21,23]		✓				
[25]	✓			✓		✓
[28]	✓			✓		✓
[38]		✓		✓	✓	✓
Ours	✓	✓	✓	✓	✓	✓

To detect fires in a timely manner, a simple yet effective method is to increase the number of UAVs and the times they are dispatched within a specific area. However, the number of available UAVs is typically constrained by cost and the specific task. For example, a long patrol distance will result in a long waiting time for the same UAV to be dispatched again. In the case where the number of available UAVs is fixed, an alternative is to minimize the patrol distance so that the frequency of dispatch is increased within a certain time interval. Meanwhile, the percentage of high fire risk areas patrolled should be maximized. Ideally, the UAV patrol path could improve the travel time in high-fire-risk areas without losing the overall detection coverage. Therefore, fire risk information, patrol distance, and dispatch frequency should be jointly considered when planning patrol paths

for UAV-based early fire detection. However, such factors have not been well considered in this type of patrol path planning. Moreover, one of the main problems in planning an appropriate cruise path is that the UAV can cruise the target area with little detour, and then return to the initial position within its maximum cruise distance.

In this paper, we propose a risk-specific patrol path (RSUPP) approach for planning an optimal UAV patrol path that integrates distance, large area suitability, and fire risk. We show that the fire risk map can be exploited to optimize the UAV patrol path. In addition, since it is difficult for a single UAV to complete the task of patrolling a long path in a large forest area within its maximum cruise distance, this approach requires the cooperation of multiple UAVs. Thus, large areas will be divided into smaller subareas, such that single UAVs can finish their patrol task in the subareas. Meanwhile, in order to perform specific fire detection patrol tasks for different fire risk areas (for example, when the number of patrol times varies with the fire risk), RSUPP applies a novel strategy.

RSUPP clusters fire risk areas with the Gaussian mixture clustering algorithm. For example, very-high-fire-risk areas (points) were clustered and divided into smaller subareas. This made the very-high-fire-risk points in the subareas dense; consequently, the point-to-point distance between any pair of points was relatively shorter. Then, the points with the same fire risk were input into the RSOM path planning algorithm to obtain the shortest path for the UAV in a given subarea. Lastly, multiple UAVs can patrol along the shortest path of each subarea within their maximum cruise distance. The workflow of this method is shown in Figure 1.

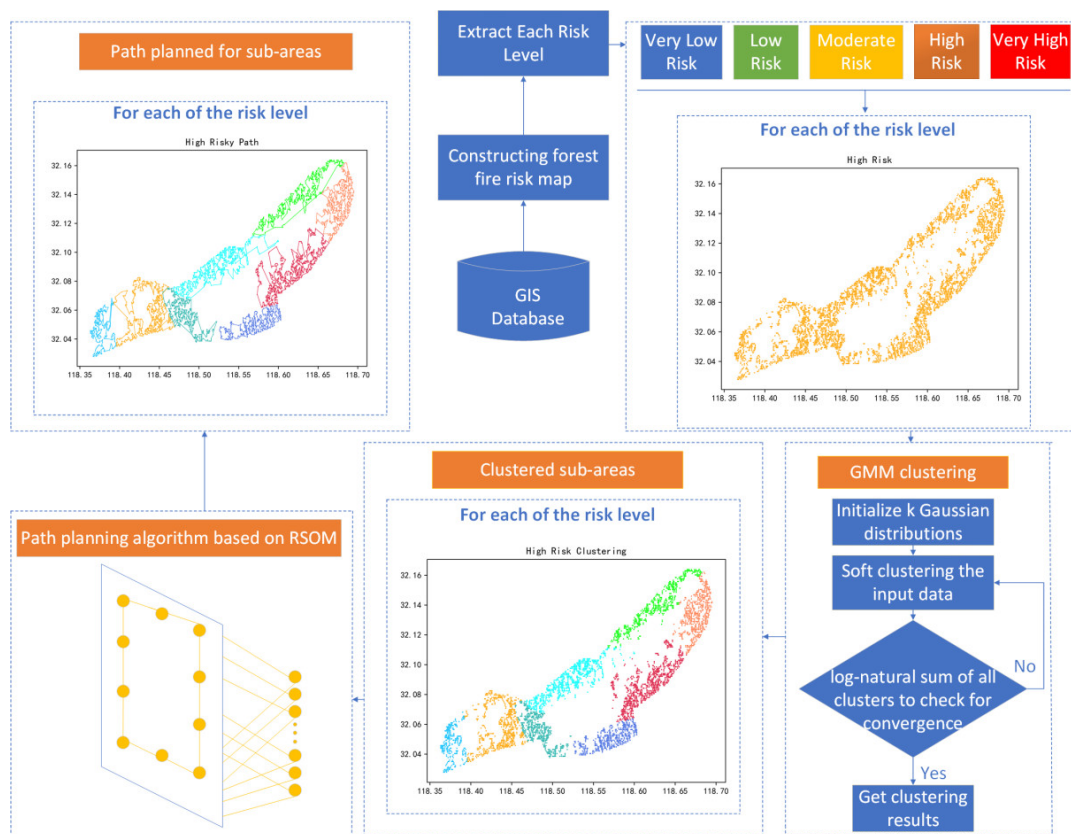


Figure 1. Flowchart of proposed method.

It is worth noting that RSUPP is totally different from approaches in previous studies [39–41], in which they inputted all points for clustering regardless of the fire risk level.

In order to validate the performance of RSUPP, we evaluated it against the related RSB and LSB algorithms on a practical dataset. Since direct comparisons of the validity of these methods could be made only on the basis of the same area, we also clustered the

whole area using all points. Then, we applied the RSOM-based path planning method to the subareas obtained by clustering all points to obtain risk-specific paths of the subareas. In order to distinguish this method from RSUPP, we call it AP-RSUPP.

The evaluation results demonstrate that paths obtained by AP-RSUPP could patrol a high percentage of target points within same flight distance. The number of very-high-risk points patrolled by AR-RSUPP paths was at least 12.03% and 85.64% higher compared to the LSB and RSB paths, respectively. The total flight distance with RSUPP was approximately six-tenths the distance with AP-RSUPP at the completion of patrolling all of the very-high-risk points.

The remainder of this paper is organized as follows: Section 2 describes the proposed method. The result of the proposal is then analyzed and discussed in Section 3. Section 4 summarizes the findings and provides a conclusion.

## 2. Methods

### 2.1. Model Formulation

To devise an approach that maximizes the percentage of high-fire-risk points patrolled while minimizing the total distance along the points, the following objective function, constraints, and decision variables were used in the model formulation:

$$\min D = \sum_i \sum_j d_{ij} p_{ij}, \quad (1)$$

$$\max R = \sum_i \sum_j p_{ij}, \quad (2)$$

$$p_{ij} = \begin{cases} 1 & \text{if the solution to TSP from point } i \text{ to point } j \\ 0 & \text{otherwise} \end{cases} \quad (3)$$

$$\sum_{i=1}^{i=N} p_{ij} = 1 \text{ (for } j = 1, 2, \dots, N), \quad (4)$$

$$\sum_{j=1}^{j=N} p_{ij} = 1 \text{ (for } i = 1, 2, \dots, N), \quad (5)$$

$$u_i - u_j + N p_{ij} \leq N - 1 \text{ (for } i \neq j, i = 2, 3, \dots, N; j = 2, \dots, N), \quad (6)$$

All  $p_{ij} = 0$  or  $1$ , All  $u_j > 0$ .

Objective Function (1) is used to minimize the total distance of all patrolled target points. Objective Function (2) is used to maximize the points of fire risk being patrolled. Constraint (3) indicates whether each point has been visited. Constraints (4) and (5) ensure that each point is patrolled only once. Constraint (6) guarantees that all points have a complete loop and that there are no subloops.

### 2.2. Gaussian Mixture Model

In this study, the whole area was clustered using the Gaussian mixture model such that a large area was divided into several subareas for patrolling. The Gaussian mixture model is a common clustering algorithm that is formed by the linear combination of multiple single Gaussian models [42]. The model assumes that all samples obey mixed normal distribution and estimates the probability density function of the samples. The model obtained is a linear combination of Gaussian models, with one cluster corresponding to one Gaussian distribution. Coordinate points are input, and, after initialization, the responsivity of multiple single Gaussian models to points is calculated, before iterating the parameters of each model. The iterated parameters are then used to calculate the membership degree of each model. For each point, the model subscript with the highest responsivity is regarded as its category identification, and the category to which the point belongs is obtained.

1. Initialize  $k$  Gaussian distributions with random mean  $\mu$  and random variance  $\sigma^2$  for each Gaussian distribution.
2. Perform soft clustering on the input data (known as the expectation step), and calculate the membership degree of each coordinate point to each category with Equation (7).

$$E = \frac{N(X_i|\mu_1, \sigma_1^2)}{N(X_i|\mu_1, \sigma_1^2) + N(X_i|\mu_2, \sigma_2^2) + \dots + N(X_i|\mu_l, \sigma_l^2)}, \quad (7)$$

where  $N(X|\mu, \sigma^2)$  is the probability density function of the normal distribution (Equation (8)), and the value range of  $l$  is  $1, 2, 3, \dots, K$ .

$$N(X|\mu, \sigma^2) = \frac{1}{(2\pi\sigma^2)^{1/2}} e^{-\frac{1}{2\sigma^2}(x - \mu)^2}. \quad (8)$$

3. With  $E$ , estimate the parameter mean  $\mu$  and variance  $\sigma^2$  of the Gaussian distribution;  $\mu$  is the weighted average of all coordinate points calculated with Equation (9), and variance  $\sigma^2$  is calculated with Equation (10).

$$\mu_m = \frac{\sum_{i=1}^N E(Z_{ij}) X_i}{\sum_{i=1}^N E(Z_{ij})}. \quad (9)$$

$$\sigma_m^2 = \frac{\sum_{i=1}^N E(Z_{il})(X_i - \mu_l)^T}{\sum_{i=1}^N E(Z_{il})}. \quad (10)$$

4. Evaluate the log likelihood with Equation (11) to check for convergence by summing the log-likelihood values of all clusters. If there is convergence, return the result; otherwise, return to step 2.

$$\ln P(X|\mu, \sigma^2) = \sum_{i=1}^N \ln \left( \sum_{k=1}^N \pi_k N(X_i|\mu_k, \sigma_k^2) \right), \quad (11)$$

where  $\pi_k$  is the mixing coefficient.

### 2.3. Ring Self-Organizing Map-Based Path Planning

Let us consider a common application scenario of forest fire monitoring. There are  $N$  points in the areas that should be patrolled. When a UAV is used for patrolling, it is necessary to find a closed loop so that the UAV passes each point only once and the total distance is the shortest. In other words, we want to traverse all points starting from and returning to the takeoff point, and the total distance that the UAV passes can be calculated using Equation (12).

$$f_{dist} = \sum_{i=1}^{n-1} d(s_i, s_{i+1}) + d(s_n, s_1), \quad (12)$$

where  $s_i$  is the number of points, and the value is  $[1, n]$ , and  $d(s_i, s_{i+1})$  represents the distance between points  $s_i$  and  $s_{i+1}$ . Thus, this can be regarded and solved as the traveling salesman problem (TSP).

The ring self-organizing map (RSOM) algorithm was used for path optimization [43]. The algorithm is an unsupervised self-learning competitive neural network. The features of the input data can be extracted by the algorithm. The principle is to get the nearest neuron of the current node, which is called the winning neuron, and then use this neuron to create a Gaussian distribution and update the positions of other neurons successively, i.e., to update the output neuron weight vector. After iterations, the output neurons continue to learn the features behind the input data. When RSOM is applied to TSP, each node in the input layer can be seen as a point. The weights of neurons in the output layer and the output layer are in the same dimension, which indicates the

location of neurons. The requirement is to proceed from the starting point only once through each node, and finally return to the starting point. Therefore, the output layer is a ring structure. After the formation of the ring results, the neurons compete to win in the training process. Algorithm 1 shows the path planning process of RSOM method.

---

**Algorithm 1:** Path planning algorithm based on RSOM

---

```

1: ▷Input: Tmax, nums, N, C, W
2: ▷Tmax: Number of iterations
3: ▷Nums: Number of classified points
4: ▷C: Counter for each neuron
5: ▷W: Weight of each neuron
6: ▷Tint: Check time interval
7:▷Output: Path
8: i = 0, j = 1
9: While (i < Tmax) do
10:   for j = 1 to Nums do
11:     NeuronIndex = minDistanceNeuron(sorted(distance(j,1:N)))
12:     PreNeuronIndex = getPreNeuronWithNeuronIndex()
13:     NextNeuronIndex = getNextNeuronWithNeuronIndex()
14:     W = updateParameterW(NeuronIndex,PreNeuronIndex,NextNeuronIndex)
15:     C(NeuronIndex)++
16:   end for
17: ▷Add neurons
18:   if mod(i,Tint) == 0
19:     distance1 = distance(NeuronIndex,PreNeuronIndex)
20:     distance2 = distance(NeuronIndex,NextNeuronIndex)
21:     if distance1 > distance2
22:       insertNewNeuronbetween(NeuronIndex,PreNeuronIndex)
23:     else
24:       insertNewNeuronbetween(NeuronIndex,NextNeuronIndex)
25:     end if
26:   end if
27: ▷Draw points and neuronal paths
28:   displayW(Nums, W, i)
29: end While
30: return displayPath(Nums)

```

---

### 3. Results and Discussion

#### 3.1. Results of RSOM-Based Planning

A national forest park in China with high forest fire risk was selected for the case study. In order to improve the fire prevention ability, a forest fire risk map of the area was produced in [44]. The risk rating of a forest fire was derived by using a range of factors that influence the occurrence of a fire (e.g., topography, meteorology, human activities, and vegetation data). As shown in Figure 2, the areas in the fire risk map were divided into five risk levels: very low, low, medium, high, and very high.

When planning the patrol path of the UAV, different patrolling strategies should be adopted for areas with different fire probability to save on cost. Thus, specific flight paths of UAV were planned for different risk areas.

The latitude and longitude coordinates of the grids with different risk levels in the fire risk map were extracted as patrolling points (Figure 3). Using the RSOM algorithm, the flight path map and flight distance corresponding to each point were obtained (Figure 4).

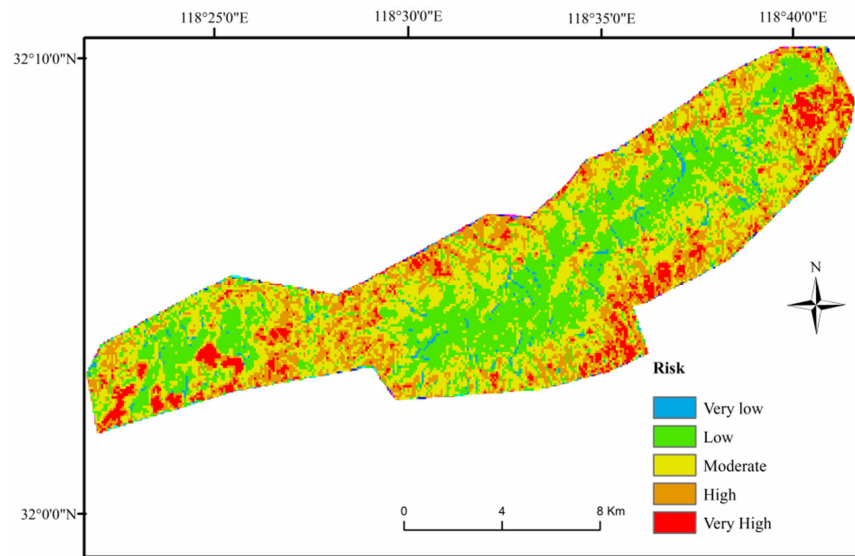


**Figure 2.** Forest fire risk map of study area.

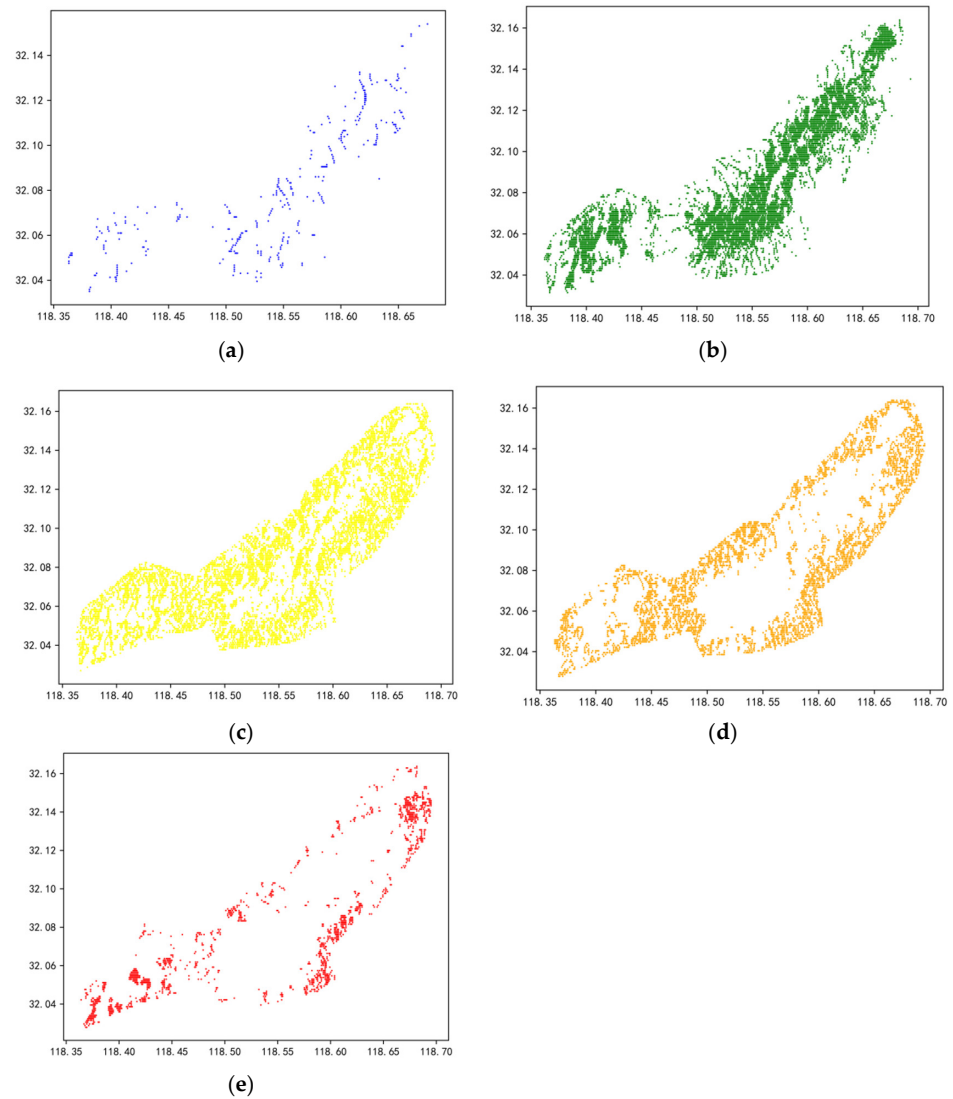


**Figure 3.** Extracted coordinates for patrolling: (a) very-low-risk area; (b) low-risk area; (c) moderate-risk area; (d) high-risk area; (e) very-high-risk area.

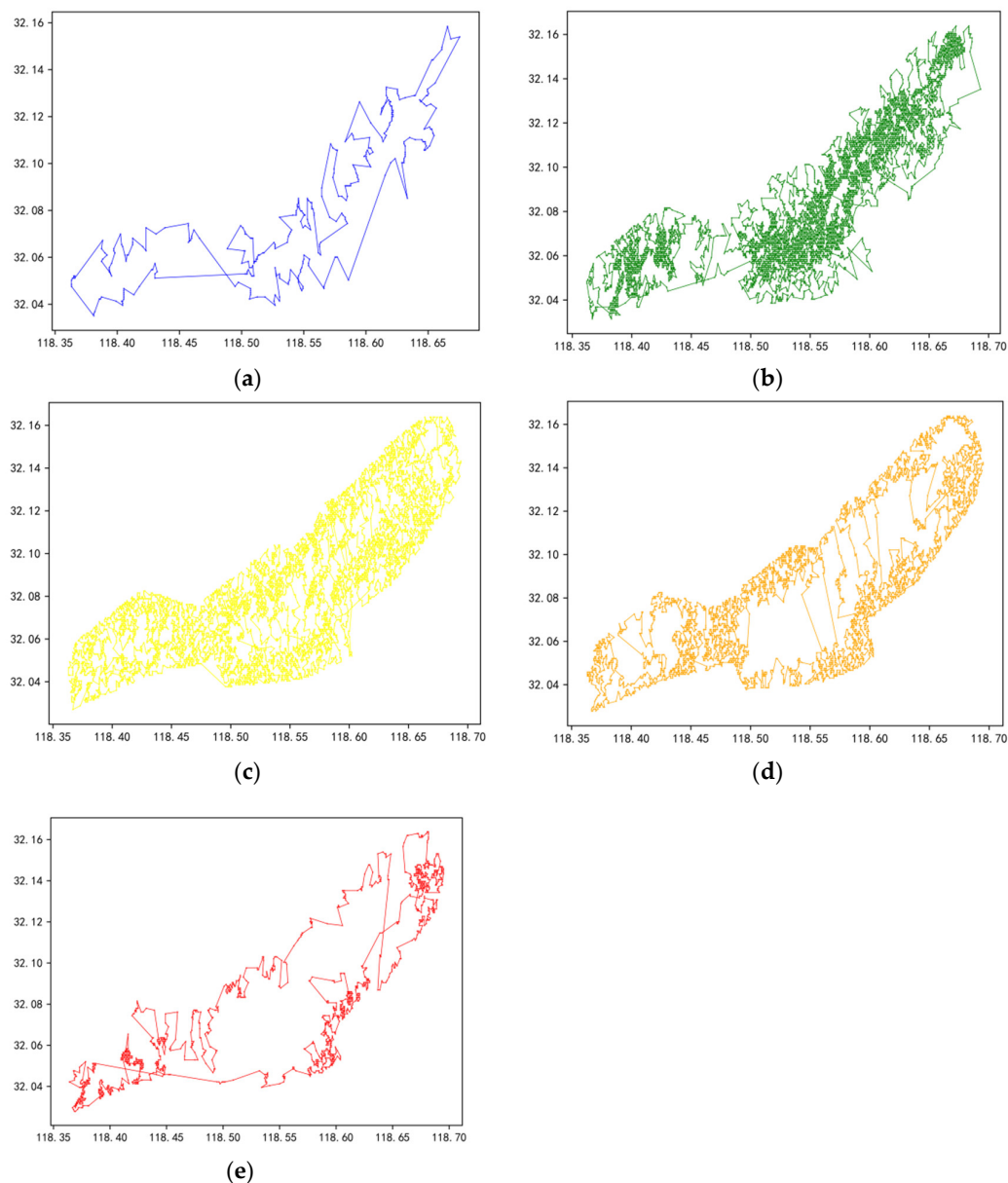


**Figure 4.** Planned paths for areas with different fire risk: (a) very low risk; (b) low risk; (c) moderate risk; (d) high risk; (e) very high risk.

Table 2 shows the flight distance and flight time corresponding to different risk levels when the flight speed of the UAV was 60 km/h. It can be seen that the flight distance and time differed in different risk areas. Among them, the moderate-risk area had the longest flight distance and flight time, 585.63 km and 9.76 h, respectively. It is difficult for a single UAV to finish the task of patrolling the long path of a large forest area within its maximum cruise distance; thus, multiple cooperating UAVs are required to patrol such a large area.

**Table 2.** Flight distance and time of single UAV.

Risk Level	Very Low	Low	Moderate	High	Very High
Distance (km)	88.96	493.79	585.63	375.48	165.00
Time (h)	1.48	8.23	9.76	6.26	2.75

### 3.2. Results of Multiple UAVs with RSUPP

Considering the endurance and time cost of a UAV, it is difficult for a single UAV to complete an entire cruise within its maximum cruise distance. Therefore, various risk areas should be patrolled by multiple UAVs. In this case, each UAV starts from a different position and takes a flight route so that only one UAV passes through each coordinate point (except the starting point). This can be regarded as the multiple traveling salesman problem (MTSP).

The vehicle routing problem (VRP) can be considered as a generalization of the MTSP. The VRP has different solutions in different application scenarios. Here, the system characteristics of the MTSP problem actually represent a special situation of the VRP [45]. That is, in an actual UAV flight situation, we need to consider the following issues [46]:

- (a) Whether the area traveled by the UAV is a fully connected graph;
- (b) Whether there is only one shortest path between any two points;
- (c) Whether the starting point coincides with the stopping point.

The TSP problem adequately describes these three issues. Moreover, denser points indicate a shorter total distance between them. Considering the UAV's cruising ability, a smaller area with relatively dense points is preferred. Thus, through Gaussian mixture model clustering, the MTSP problem was transformed into multiple independent TSP problems to satisfy the model application and requirements for cruising ability.

The fire risk maps corresponding to the study area were clustered. First, the parameters of the Gaussian mixture model were initialized and iteratively updated. Then, the final cluster classification was obtained according to the Gaussian mixture distribution. The coordinates corresponding to each category were input into the RSOM neural network to get the flight path and distance. Figure 5 shows the flight paths for multiple cooperating UAVs in the corresponding risk areas.

As mentioned above, each fire risk area was divided into patrolling subareas by Gaussian mixture model clustering; these subareas could be patrolled by multiple UAVs.

The flight distance and flight time corresponding to each subarea are listed in Table 3. The flight distance, from very low risk to very high risk, was 87.25, 492.11, 580.96, 369.01, and 163.58 km. The comparison of flight distance between a single UAV and multiple UAVs is shown in Table 4. The optimized total flight distance of multiple UAVs was slightly shorter than the distance with a single UAV. The time needed to finish the patrolling task in any risk area was greatly shortened by the cooperation of multiple UAVs. Taking the very-high-risk area as an example, it can be seen that it took 2.75 h for a single UAV to cruise once (Table 2). As shown in Table 3, when multiple UAVs carried out the cruise task simultaneously, the task could be completed within 0.57 h, which is only about one-fifth of the time required for a single UAV.

**Table 3.** Flight distance and time corresponding to each area obtained by multiple UAVs.

Sub-Area	Very Low		Low		Moderate		High		Very High	
	Distance	Time	Distance	Time	Distance	Time	Distance	Time	Distance	Time
0	13.75	0.23	67.14	1.12	90.94	1.52	48.20	0.80	34.31	0.57
1	13.13	0.22	47.70	0.80	82.61	1.38	37.50	0.63	26.27	0.44
2	11.25	0.19	73.27	1.22	30.45	0.51	26.98	0.45	23.33	0.39
3	15.01	0.25	85.69	1.43	87.77	1.46	26.98	0.45	17.25	0.29
4	9.55	0.16	70.90	1.18	67.14	1.12	68.63	1.14	14.92	0.25
5	18.91	0.32	31.49	0.52	85.09	1.42	59.31	0.99	9.93	0.17
6	2.64	0.04	55.74	0.93	80.73	1.35	55.24	0.92	10.72	0.18
7	3.01	0.05	60.18	1.00	56.23	0.94	46.17	0.77	26.85	0.45
Total distance	87.25		492.11		580.96		369.01		163.58	

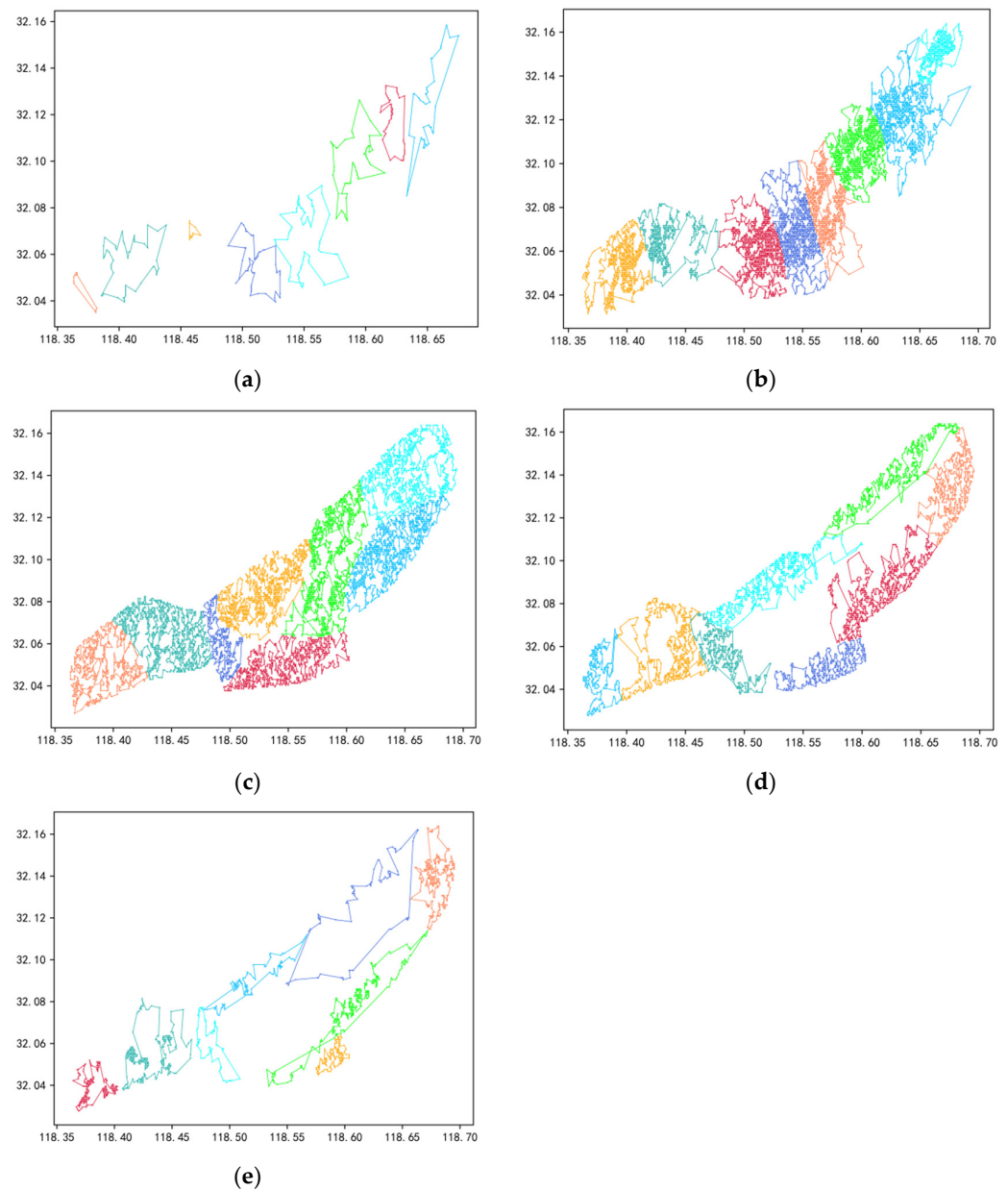


**Figure 5.** Multi-UAV paths: (a) very low risk; (b) low risk; (c) moderate risk; (d) high risk; (e) very high risk.

**Table 4.** Comparison between single and multiple UAVs.

Method	Very Low	Low	Moderate	High	Very High
	Distance (km)				
A UAV	88.96	493.79	585.63	375.48	165.00
Multi-UAV	87.25	492.11	580.96	369.01	163.58
Optimization (%)	1.9	0.3	0.7	1.7	0.8

Generally, a high fire risk level indicates that there is a high probability of fire in the area. Shortening the time for the patrolling task means that the frequency of patrolling in the area can be increased in a day. Consequently, a fire can be monitored in time, and the loss caused by fire can be reduced. For areas with different risk levels, the cruising frequency of UAVs should also be different. In this paper, the corresponding cruising

frequency was allocated according to the fire risk level, as shown in Table 5. In practice, the frequency of patrolling different risk areas can be flexibly adjusted according to the flight time and endurance of UAVs in actual situations. The total patrolling time for each subarea with multiple cooperating UAVs can be calculated using Equation (13).

$$Time_{total} = \sum_{i=1}^5 Fre_r \times Time_r, \quad (13)$$

where  $Time_{total}$  represents the total time for the UAV to cruise all risk levels in each subarea,  $Fre_r$  is the frequency of each risk level, and  $Time_r$  is the time for UAV patrolling at each risk level in each subarea.

**Table 5.** Frequency corresponding to each risk level.

Risk Level	Frequency
Very low	1
Low	2
Moderate	3
High	4
Very high	5

The control stations of the UAVs are shown in Figure 6, where P0–P7 indicate the starting positions of the UAVs. Patrolling tasks in areas with different risk levels can be completed by multiple UAVs. The longitude and latitude corresponding to the stations are shown in Table 6.

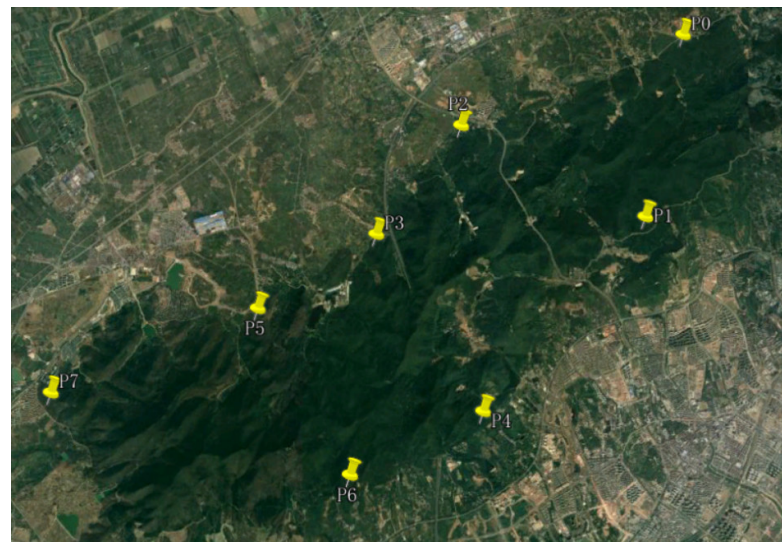


**Figure 6.** Site distribution of UAVs.

**Table 6.** Longitude and latitude corresponding to UAV sites.

Site	Latitude	Longitude
P0	32°7'51.28" N	118°37'10.41" E
P1	32°5'54.94" N	118°36'40.02" E
P2	32°6'53.23" N	118°34'24.37" E
P3	32°5'44.13" N	118°33'21.98" E
P4	32°3'54.38" N	118°34'40.50" E
P5	32°4'57.84" N	118°31'55.44" E
P6	32°3'15.76" N	118°33'4.09" E
P7	32°4'5.73" N	118°29'25.35" E

As shown in Table 7, the total cruising time for subareas 0 and 2 was 13.08 and 7.91 h, respectively. The cruising time for other subareas was about 10 h. This means that all patrolling tasks could be finished within 1 day.

**Table 7.** Total cruise time for each category when using multiple UAVs.

Subarea	Very Low	Low	Moderate	High	Very High	Total Time (h)
0	0.23	1.12	1.52	0.80	0.57	13.08
1	0.22	0.80	1.38	0.63	0.44	10.68
2	0.19	1.22	0.51	0.45	0.39	7.91
3	0.25	1.43	1.46	0.45	0.29	10.74
4	0.16	1.18	1.12	1.14	0.25	11.69
5	0.32	0.52	1.42	0.99	0.17	10.43
6	0.04	0.93	1.35	0.92	0.18	10.53
7	0.05	1.00	0.94	0.77	0.45	10.20

### 3.3. Comparison of Related Works

In order to compare the same conditions with related works, the whole area was first clustered and divided into subareas without considering the fire risk level. For each sub-area, we applied the proposed RSOM-based path planning method to obtain the risk-specific path. In order to distinguish this method from RSUPP, we call it AP-RSUPP.

We compared our work with RSB and LSB methods [38]. The proposed AP-RSUPP planned patrol paths for every fire risk level in a given subarea, and the patrols were carried out along the paths planned for the specific risk levels. For example, after traversing the path planned for high-risk areas, all of the very-high-risk points were covered. Thus, the percentage of high-fire risk-points patrolled by the AP-RSUPP path reached 100%.

In order to compare the performance under the same conditions, we used the flight distance obtained by AP-RSUPP as the limiting condition of RSB; that is, the flight distance was the same with RSB and AP-RSUPP. Table 8 shows the percentage of each risk level patrolled by RSB and AP-RSUPP paths within the same flight distance in each subarea. It can be seen that, without the fire risk information, the number of high- and very-high-risk areas patrolled was very low when there was random patrolling by RSB paths.

**Table 8.** Percentage of risk levels patrolled by RSB and UPP paths within same flight distance in each subarea.

Subarea	Very Low		Low		Moderate		High		Very High		AP-RSUPP (%)
	Distance	RSB (%)	Distance	RSB (%)							
0	16.86	7.69	80.76	7.63	128.26	9.79	86.19	8.05	39.95	8.44	100
1	21.52	0.00	133.15	3.55	134.33	4.39	64.11	3.50	25.90	6.72	100
2	12.67	6.98	71.76	3.02	112.57	3.65	72.75	4.46	19.59	2.38	100
3	8.78	0.00	77.26	12.93	110.08	13.39	93.55	12.82	56.86	14.36	100
4	13.76	18.75	71.23	12.26	86.74	9.66	75.63	13.41	43.01	10.57	100
5	20.07	3.28	159.68	3.48	129.81	3.95	71.10	2.82	30.98	3.51	100
6	17.34	13.04	81.89	11.59	83.80	11.54	52.58	9.04	32.43	10.71	100
7	22.11	2.60	133.57	3.76	155.43	4.38	85.35	3.13	33.54	2.4	100
Total distance	133.11		809.3		941.02		601.26		282.26		

With the fire risk information, the path for patrolling for fire detection can be more purposeful. A very high fire risk level indicates a high probability of fire. Therefore, we should pay more attention to areas with a very high risk level. Taking the flight distance obtained by AP-RSUPP as the limiting condition, the LSB path patrolled along the route with the higher total average local fire probability. As shown in Table 9, the percentage of very-high-risk areas patrolled by the LSB path was improved compared to RSB.

**Table 9.** Proportion of very-high-risk areas to subareas and percentage patrolled by LSB and UPP paths.

Subarea	Origin (%)	LSB (%)	AP-RSUPP (%)
0	8.49	48.10	100
1	3.97	15.13	100
2	3.77	73.81	100
3	13.21	87.97	100
4	11.68	20.33	100
5	3.55	10.53	100
6	11.10	17.86	100
7	3.84	33.6	100

From Tables 8 and 9, we can see that the number of very-high-risk fire points patrolled by AP-RSUPP paths was approximately 85.64%–97.6% higher compared to RSB paths and 12.03%–84.76% better compared to LSB paths.

From Tables 3 and 8, we can see that the total distance for traveling all very-high-risk fire points was 163.58 and 282.26 km with RUSPP and AP-RUSPP, respectively. The total patrol distance of RUSPP paths was approximately six-tenths the distance of AP-RUSPP paths at the completion of patrolling all very-high-risk points.

#### 4. Conclusions

This paper proposed a UAV flight monitoring method based on a forest fire risk map. The RSOM neural network algorithm was used to plan routes for the UAV according to fire risk levels. Considering the endurance and time cost of a UAV, it is difficult for a single UAV to complete the whole cruise within its maximum cruise distance. Therefore, several risk areas should be patrolled with the cooperative effort of multiple UAVs. This problem can be solved by regarding it as a multiple traveling salesman problem.

Therefore, a combination of the clustering method and the RSOM distribution method was proposed to solve the path planning problem of multiple UAVs. First, the Gaussian mixture model was used to cluster risk levels, and then the respective flight paths were obtained through the RSOM neural network. When multiple UAVs were deployed cooperatively to complete the patrolling task, the maximum time required for each single UAC was shortened. The simulation results showed that the proposed method can be used to plan the paths, and the patrolling tasks can be completed within a reasonable time.

**Author Contributions:** Y.X., J.L. and F.Z. contributed equally to each and every stage of this research work. All authors have read and agreed to the published version of the manuscript.

**Funding:** This work was supported in part by Start-up Fund for New Talented Researchers of Nanjing Vocational University of Industry Technology [Grant No. YK22-05-03] and the Open Foundation of Industrial Software Engineering Technology Research and Development Center of Jiangsu Education Department [201050621ZK004].

**Data Availability Statement:** All data generated or presented in this study are available upon request from corresponding author. Furthermore, the models and code used during the study cannot be shared at this as the data also form part of an ongoing study.

**Conflicts of Interest:** The authors declare no conflict of interest.

#### References

1. Mohsen, N.; Rizeei, H.M.; Ramezani, F. Forest fire risk prediction: A spatial deep neural network-based framework. *Remote Sens.* **2021**, *13*, 2513.
2. Ertugrul, M.; Varol, T.; Ozel, H.B.; Cetin, M.; Sevik, H. Influence of climatic factor of changes in forest fire danger and fire season length in Turkey. *Environ. Monit. Assess.* **2021**, *193*, 28. [[CrossRef](#)]
3. Jain, M.; Saxena, P.; Sharma, S.; Sonwani, S. Investigation of forest fire activity changes over the central India domain using satellite observations during 2001–2020. *GeoHealth* **2021**, *5*, e2021GH000528. [[CrossRef](#)]

4. Xu, N.; Rangwala, S.; Chintalapudi, K.K.; Ganesan, D.; Broad, A.; Govindan, R.; Estrin, D. A wireless sensor network for structural monitoring. In Proceedings of the 2nd International Conference on Embedded Networked Sensor Systems, Baltimore, MD, USA, 3–5 November 2004; pp. 13–24.
5. Mao, G.; Fidan, B.; Anderson, B.D.O. Wireless sensor network localization techniques. *Comput. Netw.* **2007**, *51*, 2529–2553. [[CrossRef](#)]
6. Dampage, U.; Bandaranayake, L.; Wanasinghe, R.; Kottahachchi, K.; Jayasanka, B. Forest fire detection system using wireless sensor networks and machine learning. *Sci. Rep.* **2022**, *12*, 46. [[CrossRef](#)]
7. Bao, S.; Xiao, N.; Lai, Z.; Zhang, H.; Kim, C. Optimizing watchtower locations for forest fire monitoring using location models. *Fire Saf. J.* **2015**, *71*, 100–109. [[CrossRef](#)]
8. Heyns, A.M.; du Plessis, W.; Curtin, K.M.; Kosch, M.; Hough, G. Analysis and Exploitation of Landforms for Improved Optimisation of Camera-Based Wildfire Detection Systems. *Fire Technol.* **2021**, *57*, 2269–2303. [[CrossRef](#)]
9. Andries, H.; du Warren, P.; Michael, K.; Gavin, H. Optimisation of tower site locations for camera-based wildfire detection systems. *Int. J. Wildland Fire* **2019**, *28*, 651–665.
10. Khan, A.; Gupta, S.; Gupta, S.K. Multi-hazard disaster studies: Monitoring, detection, recovery, and management, based on emerging technologies and optimal techniques. *Int. J. Disaster Risk Reduct.* **2020**, *47*, 101642. [[CrossRef](#)]
11. Zhao, L.; Shi, Y.; Liu, B.; Hovis, C.; Duan, Y.; Shi, Z. Finer classification of crops by fusing UAV images and Sentinel-2A data. *Remote Sens.* **2019**, *11*, 3012. [[CrossRef](#)]
12. Alsamhi, S.H.; Shvetsov, A.V.; Kumar, S.; Shvetsova, S.V.; Alhartomi, M.A.; Hawbani, A.; Nyangaresi, V.O. UAV computing-assisted search and rescue mission framework for disaster and harsh environment mitigation. *Drones* **2022**, *6*, 154. [[CrossRef](#)]
13. Roberge, V.; Tarbouchi, M.; Labonté, G. Fast Genetic Algorithm Path Planner for Fixed-Wing Military UAV Using GPU. *IEEE Trans. Aerosp. Electron. Syst.* **2018**, *54*, 2105–2117. [[CrossRef](#)]
14. Lindner, G.; Schraml, K.; Mansberger, R.; Hübl, J. UAV monitoring and documentation of a large landslide. *Appl. Geomat.* **2016**, *8*, 1–11. [[CrossRef](#)]
15. Onishi, M.; Ise, T. Explainable identification and mapping of trees using UAV RGB image and deep learning. *Sci. Rep.* **2021**, *11*, 903. [[CrossRef](#)]
16. Zhao, Y.; Zheng, Z.; Liu, Y. Survey on computational-intelligence-based UAV path planning. *Knowl.-Based Syst.* **2018**, *158*, 54–64. [[CrossRef](#)]
17. Yin, C.; Xiao, Z.; Cao, X.; Xi, X.; Yang, P.; Wu, D. Offline and online search: UAV multiobjective path planning under dynamic urban environment. *IEEE Internet Things J.* **2017**, *5*, 546–558. [[CrossRef](#)]
18. Elkhrachy, I. Accuracy assessment of low-cost Unmanned Aerial Vehicle (UAV) photogrammetry. *Alex. Eng. J.* **2021**, *60*, 5579–5590. [[CrossRef](#)]
19. Arca, D.; Hacisalihoğlu, M.; Kutoğlu, Ş.H. Producing forest fire susceptibility map via multi-criteria decision analysis and frequency ratio methods. *Nat. Hazards* **2020**, *104*, 73–89. [[CrossRef](#)]
20. Alemayehu, T.S.; Kim, J.H. Efficient nearest neighbor heuristic TSP algorithms for reducing data acquisition latency of UAV relay WSN. *Wirel. Pers. Commun.* **2017**, *95*, 3271–3285. [[CrossRef](#)]
21. Zhang, H.; Dou, L.; Xin, B.; Chen, J.; Gan, M.; Ding, Y. Data collection task planning of a fixed-wing unmanned aerial vehicle in forest fire monitoring. *IEEE Access* **2021**, *9*, 109847–109864. [[CrossRef](#)]
22. He, L.; Aouf, N.; Song, B. Explainable Deep Reinforcement Learning for UAV autonomous path planning. *Aerosp. Sci. Technol.* **2021**, *118*, 107052. [[CrossRef](#)]
23. Zhou, J.; Zhang, W.; Zhang, Y.; Zhao, Y.; Ma, Y. Optimal Path Planning for UAV Patrolling in Forest Fire Prevention. In *Asia-Pacific International Symposium on Aerospace Technology*; Springer: Singapore, 2018; pp. 2209–2218.
24. Amiri, M.; Pourghasemi, H.R. Predicting areas affected by forest fire based on a machine learning algorithm. *Comput. Earth Environ. Sci.* **2022**, 351–362.
25. Li, M.; Richards, A.; Sooriyabandara, M. Reliability-Aware Multi-UAV Coverage Path Planning using a Genetic Algorithm. In Proceedings of the 20th International Conference on Autonomous Agents and MultiAgent Systems, Online, 3–7 May 2021; pp. 1584–1586.
26. Van Hoang, T.; Chou, T.Y.; Fang, Y.M.; Nguyen, N.T.; Nguyen, Q.H.; Xuan Canh, P.; Ngo Bao Toan, D.; Nguyen, X.L.; Meadows, M.E. Mapping Forest Fire Risk and Development of Early Warning System for NW Vietnam Using AHP and MCA/GIS Methods. *Appl. Sci.* **2020**, *10*, 4348. [[CrossRef](#)]
27. Pan, Y.; Yang, Y.; Li, W. A deep learning trained by genetic algorithm to improve the efficiency of path planning for data collection with multi-UAV. *IEEE Access* **2021**, *9*, 7994–8005. [[CrossRef](#)]
28. Nagasawa, R.; Mas, E.; Moya, L.; Koshimura, S. Model-based analysis of multi-UAV path planning for surveying postdisaster building damage. *Sci. Rep.* **2021**, *11*, 18588. [[CrossRef](#)]
29. Gheshlaghi, A.; Hassan; Feizizadeh, B.; Blaschke, T. GIS-based forest fire risk mapping using the analytical network process and fuzzy logic. *J. Environ. Plan. Manag.* **2020**, *63*, 481–499. [[CrossRef](#)]
30. Bonazountas, M.; Kallidromitou, D.; Kassomenos, P.A.; Passas, N. Forest fire risk analysis. *Hum. Ecol. Risk Assess.* **2005**, *11*, 617–626. [[CrossRef](#)]
31. Sivrikaya, N.U.R.İ.; Saglam, B.; Akay, A.; Bozali, N. Evaluation of forest fire risk with GIS. *Pol. J. Environ. Stud.* **2014**, *23*, 187–194.

32. Jaiswal, R.K.; Mukherjee, S.; Raju, K.D.; Saxena, R. Forest fire risk zone mapping from satellite imagery and GIS. *Int. J. Appl. Earth Obs. Geoinf.* **2002**, *4*, 1–10. [[CrossRef](#)]
33. Adab, H.; Kanniah, K.D.; Solaimani, K. Modeling forest fire risk in the northeast of Iran using remote sensing and GIS techniques. *Nat. Hazards* **2013**, *65*, 1723–1743. [[CrossRef](#)]
34. Alonso-Betanzos, A.; Fontenla-Romero, O.; Guijarro-Berdiñas, B.; Hernández-Pereira, E.; Andrade, M.I.P.; Jiménez, E.; Soto, J.L.L.; Carballas, T. An intelligent system for forest fire risk prediction and fire fighting management in Galicia. *Expert Syst. Appl.* **2003**, *25*, 545–554. [[CrossRef](#)]
35. Eugenio, F.C.; dos Santos, A.R.; Fiedler, N.C.; Ribeiro, G.A.; da Silva, A.G.; dos Santos, Á.B.; Paneto, G.G.; Schettino, V.R. Applying GIS to develop a model for forest fire risk: A case study in Espírito Santo, Brazil. *J. Environ. Manag.* **2016**, *173*, 65–71. [[CrossRef](#)]
36. Sharma, L.K.; Kanga, S.; Nathawat, M.S.; Sinha, S.; Pandey, P.C. Fuzzy AHP for forest fire risk modeling. *Disaster Prev. Manag. Int. J.* **2012**.
37. Jain, A.; Ravan, S.A.; Singh, R.K.; Das, K.K.; Roy, P.S. Forest fire risk modelling using remote sensing and geographic information system. *Curr. Sci.* **1996**, *70*, 928–933.
38. Ozkan, O.; Kilic, S. UAV routing by simulation-based optimization approaches for forest fire risk mitigation. *Ann. Oper. Res.* **2022**, *314*, 1–37. [[CrossRef](#)]
39. Wang, J.; Deng, H.; Wang, C.; Cao, X. A Dual-Robot Welding Path Planning Method Based on Kmeans and Ant Colony Algorithms. In Proceedings of the 2021 8th International Conference on Information, Cybernetics, and Computational Social Systems (ICCS), Beijing, China, 10–12 December 2021; pp. 172–176.
40. Yue, X.; Zhang, W. UAV path planning based on k-means algorithm and simulated annealing algorithm. In Proceedings of the 2018 37th Chinese Control Conference (CCC), Wuhan, China, 25–27 July 2018; pp. 2290–2295.
41. Tang, Y.; Zhou, R.; Sun, G.; Di, B.; Xiong, R. A novel cooperative path planning for multirobot persistent coverage in complex environments. *IEEE Sens. J.* **2020**, *20*, 4485–4495. [[CrossRef](#)]
42. He, X.; Cai, D.; Shao, Y.; Bao, H.; Han, J. Laplacian regularized gaussian mixture model for data clustering. *IEEE Trans. Knowl. Data Eng.* **2010**, *23*, 1406–1418. [[CrossRef](#)]
43. Sasamura, H.; Ohta, R.; Saito, T. A simple learning algorithm for growing ring SOM and its application to TSP. In Proceedings of the 9th International Conference on Neural Information Processing, Singapore, 18–22 November 2002; Volume 3, pp. 1287–1290.
44. Zhao, P.; Zhang, F.; Lin, H.; Xu, S. GIS-Based Forest Fire Risk Model: A Case Study in Laoshan National Forest Park, Nanjing. *Remote Sens.* **2021**, *13*, 3704. [[CrossRef](#)]
45. Conway, R.W.; Johnson, B.M.; Maxwell, W.L. Some problems of digital systems simulation. *Manag. Sci.* **1959**, *6*, 92–110. [[CrossRef](#)]
46. Chen, T.; Zhang, G.; Hu, X.; Xiao, J. Unmanned aerial vehicle route planning method based on a star algorithm. In Proceedings of the 2018 13th IEEE Conference on Industrial Electronics and Applications (ICIEA), Wuhan, China, 31 May–2 June 2018; pp. 1510–1514.